Analyst

Cite this: *Analyst*, 2011, **136**, 3803

www.rsc.org/analyst

PAPER

Superoxide radical biosensor based on a nano-composite containing cytochrome c

Parvaneh Rahimi,[ab] Hedayatollah Ghourchian*[a] and Hossain-Ali Rafiee-Pour[ac]

Received 4th May 2011, Accepted 23rd June 2011
DOI: 10.1039/c1an15380c

A biosensor for the quantification of superoxide radical ($O_2^{\cdot-}$) was developed based on a nano-composite containing cytochrome c (Cyt c), carboxylated multi-walled carbon nanotubes and a room temperature ionic liquid (RTIL). The immobilized Cyt c was characterized by field emission scanning electron microscopy, electrochemical impedance spectroscopy and cyclic voltammetry. Using this biosensor a formal potential of −280 mV (*vs.* Ag/AgCl) and electron transfer rate constant of 1.24 was recorded for the immobilized Cyt c in 0.1 M phosphate buffer solution (pH 7.0). The biosensor showed a relatively high sensitivity (7.455 A M^{-1} cm^{-2}) and a long term stability (180 days) towards $O_2^{\cdot-}$ in the concentration range from 0.05 to 8.1 μM with a detection limit of 0.03 μM. The selectivity of the biosensor to $O_2^{\cdot-}$ was verified when its response was compared with those obtained by four potential interfering substances (ascorbic acid, uric acid, acetaminophen and hydrogen peroxide).

Introduction

The superoxide radical ($O_2^{\cdot-}$) is a biologically reactive oxygen species deployed by the immune system to kill invading microorganisms. Excessive concentration of $O_2^{\cdot-}$ not only damages many biological molecules, but also is converted to other more toxic radicals such as H_2O_2, $HO^{\cdot}$ and $^1O_2$.[1] Over the past decade, different methods have been used to detect $O_2^{\cdot-}$. Bioelectrochemical quantifications of $O_2^{\cdot-}$ have received extensive attention because they can be easily incorporated into portable analytical devices. The electrochemical $O_2^{\cdot-}$ biosensing is based on either superoxide dismutase (SOD) or cytochrome c (Cyt c) modified electrodes.[2] Application of SOD modified electrodes for $O_2^{\cdot-}$ biosensing often suffers from a lack of reproducibility due to immobilization problems. On the contrary, $O_2^{\cdot-}$ biosensors based on Cyt c modified electrodes are more stable.[3]

Carbon nanotubes (CNTs), due to their unique structure, remarkable electronic, mechanical and chemical properties, have been used as electrode mediators to accelerate electron-transfer between the matrix electrode and redox proteins/enzymes.[4,5] Recent studies demonstrated that the surface chemistry of CNTs not only alters the extent of protein coverage but also affects the conformation and activity of adsorbed proteins. Oxidative treatment on MWCNTs and creation of COOH functional groups using either concentrated HNO_3 or a mixture of concentrated H_2SO_4 and HNO_3[6] and also creation of other functional groups on CNTs[7,8] could improve protein adsorption/immobilization onto the CNT surface.

Application of room-temperature ionic liquids (RTIL), due to their ionic nature could facilitate the direct electrochemistry of proteins/enzymes.[9,10] This could provide a basis for developing biosensors, biomedical devices, bio-fuel cells, *etc.*[4,11,12] RTILs composed of a kosmotropic anion and chaotropic cation could play an important role in the stabilizing of proteins.[13] Among various RTILs-related composites, carbon nanotube-RTIL nano-composites have attracted considerable attention. Electrodes modified by carbon nanotube-RTIL composites and heme-containing proteins/enzymes have been reported in a number of articles. But, these studies were performed in different ways. Therefore, the obtained results are not comparable to each other and some conflicting data even exist.[4,12] Efforts continue to understand the mechanism by which RTILs improve the direct electrochemistry of proteins.

In the present study, a nano-composite containing Cyt c, carboxylated multi-wall carbon nanotubes (MWCNTs) and a RTIL was produced. Then a glassy carbon (GC) electrode was modified using this nano-composite. The modified electrode was first characterized *via* field emission scanning electron microscopy (FESEM). Then, it was used to describe the direct electrochemical behavior of Cyt c. Finally, the proposed electrode was used as a biosensor for quantification of $O_2^{\cdot-}$. The results revealed a higher sensitivity when compared with the data obtained by biosensors reported in the literature.

[a]*Laboratory of Microanalysis, Institute of Biochemistry and Biophysics, University of Tehran, Tehran, Iran. E-mail: hadi@ibb.ut.ac.ir; Fax: +98 21 66404680; Tel: +98 21 66408920*
[b]*Center of Excellence in Electrochemistry, Faculty of Chemistry, University of Tehran, Tehran, Iran*
[c]*Department of Biotechnology, Faculty of Science, University of Kashan, P.O. Box, 78317-51167 Kashan, Iran*

Experimental

Reagents

Horse heart Cyt c was purchased from Sigma and used without further purification. 1-Allyl-3-methylimidazolium bromide (AMI-Br) as a typical RTIL was purchased from Sigma. MWCNTs (diameter 8–15 nm, length 50 μm), prepared by chemical vapor deposition, were supplied by Timesnano Co. (China). $K_4[Fe(CN)_6]$, $K_3[Fe(CN)_6]$, KCl, KH_2PO_4, K_2HPO_4, DMSO and NaOH were obtained from Merck. All solutions were prepared in double-distilled de-ionized water.

The superoxide radical was prepared using a simple and efficient method.[14,15] Briefly, oxygen was bubbled in DMSO for 5 min. Then by addition of distilled water, DMSO was diluted to a 10% (v/v) solution. Subsequently, NaOH was added to the solution up to a final concentration of 5 mM. Finally, based on the $O_2^{\cdot-}$ molar extinction coefficient in DMSO (2006 L mol^{-1} cm^{-1} at 271 nm),[15] its concentration was estimated to be 0.047 mM. The thus prepared solution of $O_2^{\cdot-}$ in DMSO was stored with a molecular sieve with pore size of 4 Å in order to remove the excess water molecules. When the alkaline DMSO was kept in a tightly stoppered vessel at room temperature, a slow decreasing of the superoxide concentration was observed in the first 30 min. Then, the solutions were found to be very stable and no further decay was observed within 24 h.[15]

Apparatus

Electrochemical studies were carried out using an electrochemical system (EG&G model 263A potentiostat/galvanostat) controlled by a PowerSuite software package and a GPIB interface. All electrochemical studies were carried out using a conventional three-electrode cell equipped with a working GC electrode (bare or modified with nano-composite film, from Azar Electrode, Uromia, Iran), a saturated silver/silver chloride (Ag/AgCl) reference electrode (from Metrohm), and a platinum wire counter electrode. All potentials were measured and reported *versus* the Ag/AgCl reference electrode and the electrochemical experiments were carried out at 25 ± 1 °C. Electron microscope images were obtained using a FESEM model S4160, Hitachi, Japan. Electrochemical impedance measurements were carried out in 0.1 M KCl containing 2 mM $K_4[Fe(CN)_6]/K_3[Fe(CN)_6]$ (1 : 1) using a PGSTAT30/FRA2 system (Autolab, The Netherlands). The amplitude of the applied sinusoidal wave potential in each case was 5 mV. The sonication was carried out using an ultrasonic bath (Techno-Gaz, Italy).

Preparation of the modified electrode

Prior to coating, the GC electrode (2 mm in diameter) was polished with 0.3 and 0.05 μm alumina slurry, respectively, and then sonicated in de-ionized water.

In order to purify the MWCNTs and introduce carboxylic groups onto the MWCNTs' surfaces, they were chemically oxidized with HNO_3 35% at 40 °C under sonication for 5 h. Then, 2 mg of carboxylic acid functionalized MWCNTs (HOOC-MWCNTs) was dispersed in 1 mL of AMI-Br by grinding them in an agate mortar for about 1 h. The suspensions were centrifuged at 12,000 rpm for 30 min. At that time, a black nanocomposite of HOOC.MWCNTs-RTIL would be formed. Using a micropipette the supernatant was removed and the black nanocomposite was collected and dispersed in 1 mL of double-distilled water. Then, 2 μL of the suspension was thoroughly mixed with 2 μL of Cyt c solution (8 mg mL^{-1} in phosphate buffer solution, PBS, pH 7.0). Finally, 2 μL of the mixture was dropped on the GC electrode surface. Then the solvent was allowed to be evaporated at room temperature. The modified electrode was denoted as a Cyt c-HOOC.MWCNTs-RTIL/GC electrode.

Results and discussion

Characterization of the Cyt c-HOOC.MWCNT-RTIL/GC electrode

The surface topography of the modified electrodes including HOOC.MWCNTs (A), HOOC.MWCNTs-RTIL (B) and Cyt c-HOOC.MWCNTs-RTIL/GC (C) were investigated by FESEM (Fig. 1). Fig. 1A represents the homogeneous cylindrical morphology of functionalized MWCNTs, while entangled to each other. But as observed in Fig. 1B, by addition of RTIL to the HOOC.MWCNTs, a mass of RTIL has been embedded into the gaps of the HOOC.MWCNTs and uniformly integrated with them. When the Cyt c was immobilized on the relatively uniform surface of the HOOC.MWCNTs-RTIL, a significant change in the surface morphologies of the modified electrode appeared (Fig. 1C). This clearly revealed the successful adsorption of the protein on the HOOC.MWCNTs-RTIL film.

Electrochemical impedance spectroscopy (EIS) was employed to provide useful information during the electrode surface modification process. Fig. 1D displays the typical Nyquist plots ($-Z''$ *vs.* Z') of different electrodes in the frequency range from 10^{-2} to 10^5 Hz. As seen, the resistance of the bare GC electrode (Curve **a**) is more than that of the HOOC.MWCNTs-RTIL/GC

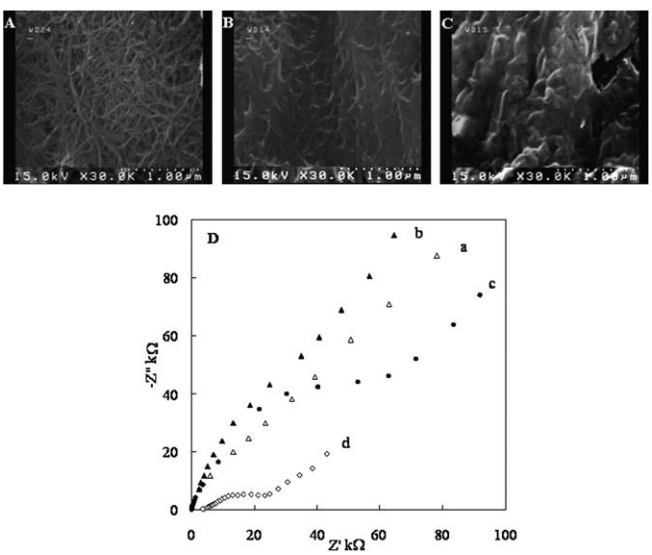

Fig. 1 A–C, the FESEM images of HOOC.MWCNTs/GC, HOOC.MWCNTs-RTIL/GC, and Cyt c-HOOC.MWCNTs-RTIL/GC electrodes, respectively. D, the electrochemical impedance spectra of (a) bare GC, (b) HOOC.MWCNTs-RTIL/GC, (c) Cyt c/GC and (d) Cyt c-HOOC.MWCNTs-RTIL/GC electrodes in 0.1 M KCl solution containing 2 mM $K_3[Fe(CN)_6]/K_4[Fe(CN)_6]$.

electrode (Curve **b**). Comparison of Curves **a** and **b** reveals that the HOOC.MWCNTs-RTIL nano-composite was obviously able to decrease the interfacial electron transfer resistance at the bare GC electrode. In the next experiments, when Cyt c was coated on the surface of the bare GC electrode (Curve **c**), the EIS of the resulting electrode showed an obvious semicircle domain with a diameter of about 63 kΩ. The semicircle diameter is a criterion corresponding to the electron-transfer resistance. But, the presence of the HOOC.MWCNTs-RTIL nano-composite between Cyt c and the GC electrode could decrease the resistance to ~23 kΩ (Curve **d**). This indicated that the Cyt c molecules blocked the pathway of electron transfer, but the HOOC. MWCNTs-RTIL nano-composite was obviously able to re-establish the electron transfer pathway at the bio-sensing interface.

Direct electrochemistry of Cyt c on the HOOC.MWCNTs-RTIL/GC electrode

To evaluate the electrochemical performance of Cyt c immobilized on the HOOC.MWCNTs-RTIL/GC electrode, cyclic voltammetry was used. Cyclic voltammograms (CVs) of different modified electrodes in 0.1 M N_2-saturated PBS, pH 7.0 at the scan rate of 0.1 V s^{-1} were recorded (Fig. 2A). As can be seen, when Cyt c is adsorbed on either a bare or RTIL modified GC electrode, it showed no response (Curves **a** and **b**, respectively). Also, no peak was observed for the HOOC.MWCNTs/GC (Curve **c**) and HOOC.MWCNTs-RTIL/GC (Curve **d**) electrodes because they contain no electroactive species. But, by adsorbing Cyt c on either the HOOC.MWCNTs/GC or HOOC.MWCNTs-RTIL/GC modified electrode, a pair of well-defined redox peaks was observed (Curves **e** and **f**, respectively). These results indicate the role of HOOC.MWCNTs in mediating the electron transfer between Cyt c and the GC electrode. The value of the formal potential [$E^{\circ\prime} = (E_{pc} + E_{pa})/2$] for Cyt c at HOOC.MWCNTs/GC electrode is −325 mV which is ~45 mV more negative than that obtained at the HOOC.MWCNTs-RTIL/GC electrode (~−280 mV), and the value of the peak-to-peak separation (ΔE_p) at scan rates below 200 mV s^{-1} for the Cyt c-HOOC.MWCNTs/GC electrode (138 mV) is larger than that for the Cyt c-HOOC. MWCNTs-RTIL/GC electrode (86 mV).

Based on these results, the reversibility of the direct electron-transfer reaction of Cyt c at the HOOC.MWCNTs-RTIL/GC electrode is higher than that obtained at the HOOC.MWCNTs/GC electrode.

As can be seen in Fig. 2B, both the reduction and oxidation peak potentials of the Fe^{III}/Fe^{II} redox couple of the Cyt c-HOOC. MWCNTs-RTIL/GC electrode was pH dependent in the pH range from 2.5 to 11.5. The Cyt c formal potential shifted negatively with the increase in pH. This observation shows that a proton is involved in the electron transfer process of Cyt c.[16] Fig. 3 shows the CVs of the Cyt c-HOOC.MWCNTs-RTIL/GC electrode in N_2-saturated PBS at different scan rates. Both the anodic and cathodic peak currents increased linearly with the scan rate change (Fig. 3A), indicating that the electrode reaction is a surface confined process. As can be observed in Fig. 3B the formal potential is almost independent of the potential scan rate for sweep rates below 300 mV s^{-1} suggesting the facile charge transfer kinetics over this range of sweep rate. However, for scan rates above 300 mV s^{-1} the peak separations begin to increase demonstrating the limitation arising from charge transfer kinetics. By using the slope of the peak current *versus* scan rate in the Laviron Equation,[17] $I_p = n^2F^2\nu A\Gamma_c/4RT$, the average surface coverage of Cyt c (Γ_c) on the HOOC.MWCNTs-RTIL and HOOC.MWCNTs films are estimated as 2.6×10^{-9} and 3.8×10^{-10} mol cm^{-2}, respectively. This shows that the average surface

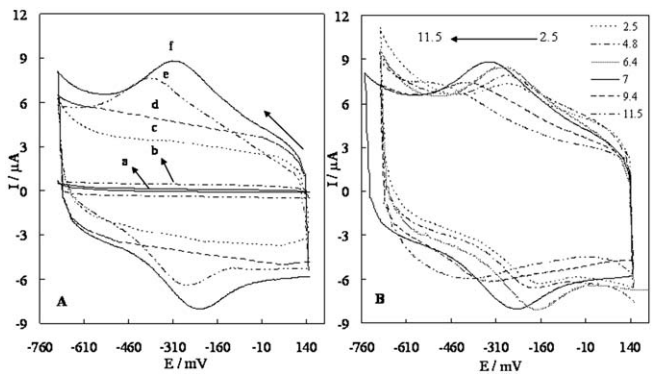

Fig. 2 A, CVs of different modified electrodes: (a) Cyt c/GC, (b) Cyt c-RTIL/GC, (c) HOOC.MWCNTs/GC, (d) HOOC.MWCNTs-RTIL/GC, (e) Cyt c-HOOC.MWCNTs/GC and (f) Cyt c-HOOC.MWCNTs-RTIL/GC electrodes. The results were obtained in 0.1 M N_2-saturated PBS, pH 7.0, at the scan rate of 0.1 V s^{-1}. B, CVs of the Cyt c-HOOC.MWCNTs-RTIL/GC electrode in 0.1 M N_2-saturated PBS at pH 2.5, 4.8, 6.4, 7.0, 9.4 and 11.5 from right to left, respectively.

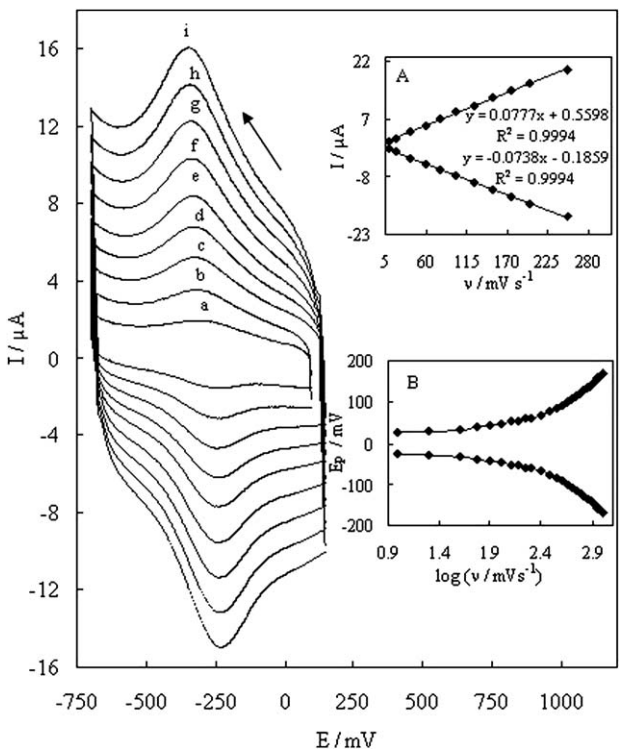

Fig. 3 CVs of the Cyt c-HOOC.MWCNTs-RTIL/GC electrode in 0.1 M N_2-saturated PBS, pH 7.0 at various scan rates of 20, 40, 60, 80, 100, 125, 150, 175 and 200 mV s^{-1} from a to i respectively. Insets represent the plots of I_p *vs.* ν (A) and E_p *vs.* log ν for scan rates from 20 to 1000 mV s^{-1} (B).

concentration of Cyt c on HOOC.MWCNTs-RTIL is about 6.8 times larger than that on HOOC.MWCNTs. The Γ_c value for Cyt c adsorption on the surface of HOOC.MWCNTs is confined to a Cyt c monolayer; while, the amount of Cyt c adsorbed on HOOC.MWCNTs-RTIL is much higher than a monolayer.[11,18] The higher Γ_c value clearly indicates that the HOOC.MWCNTs-RTIL nano-composite provides a very large active area for enzyme immobilization. As reported previously, the imidazolium ion of RTIL could interact with MWCNTs through π–π, π-cationic, hydrophobic-hydrophobic or electrostatic interactions,[11,19] also the RTIL can entrap the enzyme through multi-point enzyme-RTIL interactions (such as electrostatic, hydrogen bonds, and hydrophobic interactions) and form a supramolecular network which is able to maintain the protein structure.[20,21] Therefore, the RTIL acts as a linker between MWCNTs and Cyt c which leads to the efficient immobilization of Cyt c. The apparent charge transfer rate constant (k_s) can be estimated according to Laviron.[22] By taking a charge transfer coefficient (α) of 0.36, the k_s value obtained for Cyt c at HOOC.MWCNTs-RTIL (1.24 s^{-1} ± 0.07) was lower than that obtained at the HOOC.MWCNTs/GC electrode (3.8 s^{-1} ± 0.2). This corresponds well with the calculated values of the surface coverage of Cyt c on both modified electrodes, where the decrease in the charge transfer rate through the film could be due to the increase in protein content.[23]

Long-term stability is an essential issue for biosensors and bioreactors. Cyt c can be tightly adsorbed on the HOOC.MWCNTs-RTIL film to form a high stable modified electrode. So that after 200 continuous cycles at the scan rate of 0.1 V s^{-1}, no obvious change in CVs of Cyt c was observed (Fig. 4A).

In order to control the storage stability, the proposed modified electrode was stored at 4 °C in PBS and the CVs of Cyt c were measured at different time intervals over several months. As can be observed in Fig. 4B, the electrode retained 93% of the current response after 5 months. But at the 6th month, the decrease in the current response reached 15%. Also the electrode showed negligible change in current response towards the superoxide radical for more than 5 months. Such an excellent stability is attributed to the role of the RTIL to provide a suitable biocompatible environment for the enzyme. As reported previously, the RTIL which is a mixture of a kosmotropic anion and chaotropic cation plays an important role in protein stability.[13] In addition, the hydrogen bond capacity of the RTIL maintains the protein's native structure and bioactivity.[24] It seems the RTIL plays a crucial role in further stabilizing the protein. Therefore, the Cyt c-HOOC.MWCNTs-RTIL/GC electrode with such an outstanding stability was selected for $O_2^{\cdot-}$ detection.

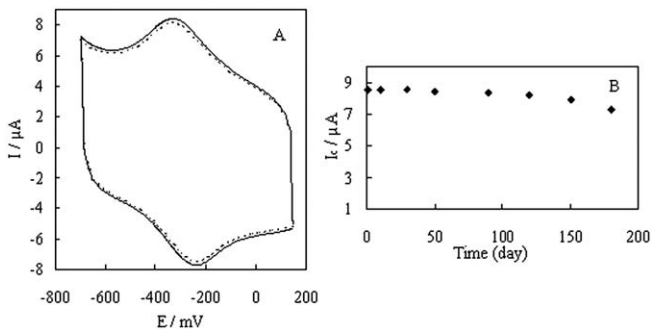

Fig. 4 A, the 1st (solid line) and 200th (dashed line) recorded CVs of the Cyt c-HOOC.MWCNTs-RTIL/GC electrode. B, variation of cathodic current during the storage time of the proposed electrode in 0.1 M PBS, pH 7.0.

Analytical characteristics of the biosensor towards $O_2^{\cdot-}$

The electrocatalytic properties of the immobilized Cyt c towards $O_2^{\cdot-}$ were investigated using linear sweep voltammetry. Fig. 5A shows the linear sweep voltammograms of $O_2^{\cdot-}$ at the Cyt c-HOOC.MWCNTs-RTIL/GC modified electrode. The reduction peak current of immobilized Cyt c increased obviously with increasing the concentration of $O_2^{\cdot-}$ in the PBS, showing a typical electrocatalytic reduction process. As shown in Reaction 1, the immobilized Cyt c was oxidized by $O_2^{\cdot-}$. On the electrode surface due to the re-reduction of Cyt c-Fe(III) (Reaction 2), a cathodic peak current can be sensed.[25]

So the increased reduction peak current of Cyt c-Fe(III) is proportional to the $O_2^{\cdot-}$ concentration.

$$\text{Cyt c-(Fe II)} + O_2^{\cdot-} + 2H^+ \rightarrow \text{Cyt c-(Fe III)} + H_2O_2 \quad (1)$$

At the electrode surface:

$$\text{Cyt c-(Fe III)} + e^- + H^+ \rightarrow \text{Cyt c-(Fe II)} \quad (2)$$

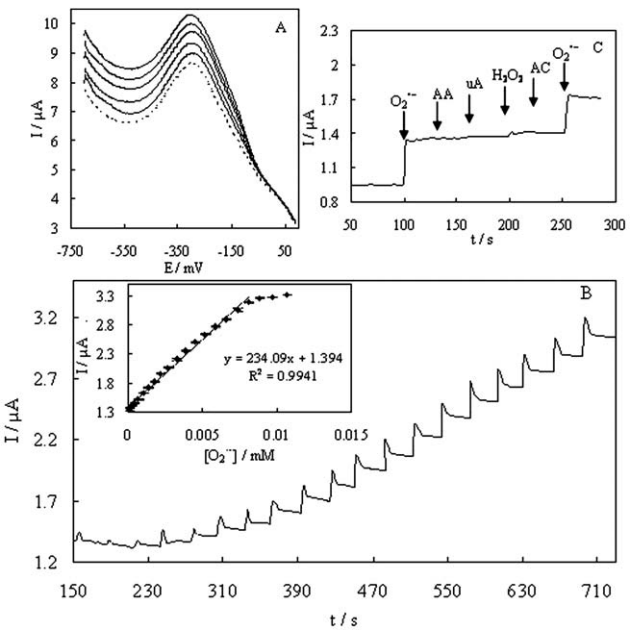

Fig. 5 A, linear sweep voltammograms of the Cyt c-HOOC.MWCNTs-RTIL/GC electrode in 0.1 M N_2-saturated PBS containing (from inner to outer) 0, 0.23, 0.29, 0.40, 0.67 and 0.86 mM $O_2^{\cdot-}$ at the scan rate of 0.1 V s^{-1}. B, amperometric response of the Cyt c-HOOC.MWCNTs-RTIL/GC electrode to $O_2^{\cdot-}$. The electrodes were held at −0.50 V (*vs.* Ag/AgCl) while its rotation speed was 500 rpm in 0.1 M PBS, pH 7.0. The final concentration of $O_2^{\cdot-}$ after each successive addition was 0.05, 0.10, 0.24, 0.42, 0.66, 0.97, 1.32, 1.74, 2.20, 2.71, 3.26, 3.85, 4.48, 5.15, 5.84, 6.56, 7.30 and 8.1 μM, respectively. The inset shows the calibration plot for $O_2^{\cdot-}$. C, response of the Cyt c-HOOC.MWCNTs-RTIL/GC electrode to 1.3 μM $O_2^{\cdot-}$, ascorbic acid (AA), uric acid (UA), acetaminophen (AC) and hydrogen peroxide (H_2O_2).

Table 1 Comparison between the analytical parameters of the proposed electrode and the others reported for $O_2^{\cdot-}$ determination

Composite	$E^{\circ\prime}$ (mV)	$K_s(s^{-1})$	Linear range(μM)	Detection limit (μM)	Sensitivity (A M^{-1} cm^{-2})	Stability (day)	Ref.
Cyt c/PASA[a]/Au	15	1.5	—	—	0. 398	2	26
DTSP[b]/Cyt c/Au	—	—	—	0.07	0.410	—	16
PTTCA[c]/Cyt c/Au	−471	0.47	0.2–2.7	0.05	0.028	15	25
Cyt c-HOOC.MWCNTs-RTIL	−280	1.24	0.05–8.1	0.03	7.455	180	This work

[a] Poly(aniline(sulfonic acid)). [b] Dithiobis(succinimidyl)propionate. [c] Poly(5,2′:5′,2″-terthiophene-3′-carboxylic acid).

Further experimental results showed that the bio-catalytic currents increased linearly with the $O_2^{\cdot-}$ concentration. The amperometric current-time curve was recorded to determine the catalytic currents of $O_2^{\cdot-}$ at the Cyt c/HOOC.MWCNTs-RTIL/GC modified electrode at −500 mV (Fig. 5B). By addition of $O_2^{\cdot-}$ into the PBS, the cathodic current reaches to the steady state within 6 s. This indicates the fast response of biosensor to $O_2^{\cdot-}$. As shown in the inset of Fig. 5B, the biosensor response is linear in the $O_2^{\cdot-}$ concentration range from 0.05 to 8.1 μM. The linear regression equation of the catalytic current *vs.* the $O_2^{\cdot-}$concentration was I_p (μA) = 234.1 [$O_2^{\cdot-}$] (mM) + 1.394 with a correlation coefficient of 0.9941 (n = 18). The current sensitivity was obtained to be 7.45 A M^{-1} cm^{-2}. The detection limit was evaluated as 0.03 μM, at the chosen probability level of 5% according to ISO 11843-2. The relative standard deviation (RSD) of the slopes of three successive calibration curves was obtained as 0.68%. The RSD of the responses of three electrodes, calculated independently using the same method, was 5.6% at 0.1 μM of $O_2^{\cdot-}$. These results indicate a reproducible immobilization process of Cyt c on the HOOC.MWCNTs-RTIL nano-composite. These values are superior to those reported in the literature (Table 1).

The apparent Michaelis–Menten constant (K_m^{ap}) is generally used to evaluate the activity of proteins. According to the Lineweaver–Burk equation,[27] the values of K_m^{ap} were estimated to be 3.6 μM. Such a low K_m^{ap} value implies that the biosensor shows a good affinity to $O_2^{\cdot-}$.

The anti-interference ability and recovery experiment

To affirm the selectivity of the proposed electrode, the effects of four potential interfering substances, including ascorbic acid (AA), uric acid (UA), acetaminophen (AC) and hydrogen peroxide (H_2O_2) were investigated. As can be seen in Fig. 5C, the detection of $O_2^{\cdot-}$ at this potential (−500 mV) is very effective and no interference was observed.

The analytical applicability of the biosensor for more complex samples was evaluated by determining the recoveries after addition of 1.3, 3.0 and 5.0 μM of $O_2^{\cdot-}$ in blood serum samples. The recovery rate of the biosensor was 101.5% (1.32 ± 0.016 μM, n = 3, RSD = 4.3%), 95% (2.85 ± 0.034 μM, n = 3, RSD = 4.1%), and 103.4% (5.17 ± 0.056 μM, n = 3, RSD = 3.7%), respectively.

Conclusions

By combination of HOOC.MWCNTs and AMI-Br as an RTIL (with great composition of kosmotropic anion and chaotropic cation) a novel nano-composite film was obtained which could serve as a suitable host matrix for Cyt c. It seems this nano-composite plays a dual role: Mainly, the MWCNTs play as a promoter for electron transfer between Cyt c and the GC electrode, while the RTIL maintains the Cyt c structure and its bioactivity. The prepared nano-composite not only could improve the direct electron transfer of Cyt c, but also provides a long-term stability for an $O_2^{\cdot-}$ biosensor. The specific behavior of the obtained biosensor towards $O_2^{\cdot-}$ and also the excellent analytical characteristics such as: high sensitivity, fast response, low detection limit, high stability and wide response range, could make the biosensor applicable for commercial purposes.

Acknowledgements

Financial supports provided by the Research Council of the University of Tehran and Iran National Science Foundation (INSF) are gratefully appreciated.

References

1 Y. XF and G. Y. Ben, *Acta Bot. Boreal-Occident Sin.*, 2000, **20**, 201–205.
2 F. Lisdat and F. W. Scheller, *Anal. Lett.*, 2000, **33**, 1–16.
3 F. Wegerich, P. Turano, M. Allegrozzi, H. Mohwald and F. Lisdat, *Anal. Chem.*, 2009, **81**, 2976–2984.
4 P. Du, S. N. Liu, P. Wu and C. X. Cai, *Electrochim. Acta*, 2007, **52**, 6534–6547.
5 J. Wang, *Electroanalysis*, 2005, **17**, 7–14.
6 Y. Wang, Z. Iqbal and S. Mitra, *J. Am. Chem. Soc.*, 2006, **128**, 95–99.
7 M. J. O'Connell, P. Boul, L. M. Ericson, C. Huffman, Y. H. Wang, E. Haroz, C. Kuper, J. Tour, K. D. Ausman and R. E. Smalley, *Chem. Phys. Lett.*, 2001, **342**, 265–271.
8 P. Du, Y. M. Shi, P. Wu, Y. M. Zhou and C. X. Cai, *Acta Chim. Sinica.*, 2007, **65**, 1–9.
9 J. S. Wilkes, J. A. Levisky, R. A. Wilson and C. L. Hussey, *Inorg. Chem.*, 1982, **21**, 1263–1264.
10 R. A. Osteryoung, R. J. Gale, J. Robinson, H. Linga and G. Cheek, *J. Electrochem. Soc.*, 1981, **128**, C79.
11 Q. Zhao, D. P. Zhan, H. Y. Ma, M. Q. Zhang, Y. F. Zhao, P. Jing, Z. W. Zhu, X. H. Wan, Y. H. Shao and Q. K. Zhuang, *Front. Biosci.*, 2005, **10**, 326–334.
12 R. T. Kachoosangi, M. M. Musameh, I. Abu-Yousef, J. M. Yousef, S. M. Kanan, L. Xiao, S. G. Davies, A. Russell and R. G. Compton, *Anal. Chem.*, 2009, **81**, 435–442.
13 M. T. Ru, S. Y. Hirokane, A. S. Lo, J. S. Dordick, J. A. Reimer and D. S. Clark, *J. Am. Chem. Soc.*, 2000, **122**, 1565–1571.
14 D. S. Shin, N. Doddapaneni and S. M. Park, *Inorg. Chem.*, 1992, **31**, 4060–4064.
15 R. F. Haseloff, B. Ebert and W. Damerau, *Anal. Chim. Acta*, 1989, **218**, 179–184.
16 C. L. Xiang, Y. J. Zou, L. X. Sun and F. Xu, *Talanta*, 2007, **74**, 206–211.
17 E. Laviron, *J. Electroanal. Chem.*, 1979, **100**, 263–270.
18 S. A. Kumar, S. F. Wang, C. T. Yeh, H. C. Lu, J. C. Yang and Y. T. Chang, *J. Solid State Electrochem.*, 2010, **14**, 2129–2135.
19 T. Fukushima and T. Aida, *Chem.–Eur. J.*, 2007, **13**, 5048–5058.
20 S. Park and R. J. Kazlauskas, *Curr. Opin. Biotechnol.*, 2003, **14**, 432–437.

21 C. F. Poole, *J. Chromatogr., A*, 2004, **1037**, 49–82.
22 E. Laviron, *J. Electroanal. Chem.*, 1979, **101**, 19–28.
23 F. Daigle and D. Leech, *Anal. Chem.*, 1997, **69**, 4108–4112.
24 P. C. A. G. Pinto, M. L. M. F. S. Saraiva and J. L. F. C. Lima, *Anal. Sci.*, 2008, **24**, 1231–1238.
25 F. Darain, J. S. Park, H. Akutsu and Y. B. Shim, *Biosens. Bioelectron.*, 2007, **23**, 161–167.
26 J. Li, S. N. Tan and H. Ge, *Anal. Chim. Acta*, 1996, **335**, 137–145.
27 M. K. Beissenhirtz, F. W. Scheller and F. Lisdat, *Anal. Chem.*, 2004, **76**, 4665–4671.

